SPACE SCIENCES LABORATORY

FINAL REPORT

for

NAS5 - 24165

Experiment Definition and Integration Study for the Accommodation of Magnetic Spectrometer Payload on Spacelab / Shuttle Missions

(June 13, 1977 - July 1, 1978)

Principal Investigator: Dr. Andrew Buffington

Series 19
Issue 45

June 27, 1978

UNIVERSITY OF CALIFORNIA, BERKELEY

Abstract: "Final Report for NAS5-24165, Experiment Definition and Integration Study for the Accommodation of Magnetic Spectrometer Payload on Spacelab/Shuttle Missions,"

Dr. Andrew Buffington
U. of California, Berkeley

This report describes a version of the super-cooled magnetic spectrometer experiment for a cosmic-ray experiment as defined for the High Energy Astronomical Observatory which may be used on a Space Shuttle Spacelab mission. Results are reported of an investigation of new cryostat parameters which are appropriate to the shuttle mission weight and mission duration constraints. Since a super-conducting magnetic spectrometer has a magnetic fringe field, a section is included which describes methods for shielding sensitive electronic and mechanical components on nearby experiments.

It seems likely that no extra shielding will be required on experiments further away than one pallet length from the magnetic spectrometer.

Space Sciences Laboratory
University of California
Berkeley, California 94720

Experiment Definition and Integration Study for the accommodation of Magnetic Spectrometer Payload on Spacelab/Shuttle Missions

Final Report for

NASA Contract NAS5-24165

June 13, 1977 - July 1, 1978

Principal Investigator: Dr. Andrew Buffington

Space Sciences Laboratory Series 19, Issue 45

TABLE OF CONTENTS

I. Introduction

Large magnetic spectrometers have been in use for many years in accelerator laboratories, but only the development of superconducting technology allowed their use in balloon-borne cosmic ray investigations. During the last decade, groups from Goddard Space Flight Center, Johnson Space Center, and the University of California at Berkeley have flown superconducting magnetic spectrometers by balloon to investigate primary cosmic rays. Table I summarizes the measurements that have been made by this technique to date; it is clear that superconducting magnetic spectrometers have made major contributions to the advancement of cosmic ray physics, and it seems likely that they will continue to do so. However, the limited exposure times afforded by balloon flights curtail many of the measurements that would be possible using this technique, and in many cases uncertainties in the corrections for overlying atmosphere cause a severe systematic uncertainty in the experimental results. Thus, it seems natural to fly such experiments by satellite, either in the "free-flyer" mode which provides maximal exposure time, or using the space shuttle "sortie" mode which provides exposures only up to a month, but with greatly reduced telemetry and command interface costs and the possibility of crew intervention.

In June 1970, the astrophysics group headed by Professor Luis W. Alvarez at Berkeley, with collaborators, proposed a cosmic-ray experiment to fly on the High Energy Astronomical Observatory (HEAO) satellite series. The experiment was to have used a superconducting magnet, spatial detectors, and scintillators to measure cosmic ray nuclei and $e^{\pm}$ and to search for antinuclei, at energies extending from the geomagnetic cutoff to about 200 GeV. The experiment passed the initial selection process and was funded through Phase B. In January 1973 the HEAO satellite program was

TABLE I

Superconducting Magnetic Spectrometer Cosmic Ray Measurements

Cosmic Ray Measurements	Results	Most Recent Publications
$Z \gtrsim 2$ Antimatter Search above 5 GV/c	none seen in ~10^5 events; this result is unlikely to be bettered without a new experimental concept.	G.F. Smoot et al., PRL 35, 258 (1975).
Primary antiprotons above 5 GeV	most stringent upper limit for $\bar{P}/P$ (3×10^{-4})	G.D. Badhwar et al., 15th Int. C.R. Conf. 1, 209 (1977).
primary $e^{\pm}$	first experiment to measure e^+ above 4 GeV; first experiment to reduce background below 10^{-5}; $e^+/(e^+ + e^-) \approx 0.1$ from 1 to 10 GeV.	A. Buffington et al., Ap. J. 199, 669 (1975); G.D. Badhwar et al., 15th Int. C.R. Conf. 1, 404 (1977).
spectra of nuclei	first to discover L/M ratio diminishes above 10 GV/c; lower systematic errors for charge and energy spectra.	C. Orth et al., submitted to Ap. J. (1978); G.D. Badhwar et al., Astr. and Spc. Sci. 28, 101 (1974).
Isotopic Measurements $3 \lesssim Z \lesssim 8$	first to discover that Be^7 drops sharply above 500 MeV/n; first to show that 2/3 of Be^{10} has decayed at high energies.	A. Buffington et al., Ap. J. (in press, to appear November 1978).

redirected, and the magnetic spectrometer experiment, because of its large size and weight requirements, had to be postponed until the space shuttle time frame. Many of the accomplishments of the phase A and phase B studies have previously been reported.[1-4] No major obstacles to the experiment have been found since that time. In particular, detailed calculations of the magnet and cryostat system[2] and tests of the charge leads[3] have established the feasibility of the original magnet and cryostat concept. Furthermore, a thermal model of the HEAO cryostat, identical in every respect to the planned flight model except for vessel wall thicknesses, has demonstrated a one-year lifetime, as predicted by the original calculations. We feel the successful thermal model demonstrations show that the original HEAO magnetic spectrometer experiment was based upon a sound cryostat design, and that such a free-flyer experiment today should have at least a one-year cryogenic lifetime.

This report describes a version of the HEAO magnetic spectrometer which is updated for the space shuttle sortie mode. This mode permits shorter flights at greatly reduced cost, and for many experiments the longer time is either unnecessary, or is required only following a series of developmental flights. In this report, we consider the possibility of flying an experiment like the HEAO one, but with the reduced cost and cryogenic lifetime constraints allowed by the space shuttle sortie mode. We consider a stripped-down experiment with a magnetic spectrometer alone, even though any real space shuttle magnetic spectrometer experiment would almost certainly include other detectors. Since these additional detectors (scintillators, Cerenkov counters, transition radiation detectors, etc.) have most likely been included in other Astronomy Spacelab Payload studies, we have elected to concentrate in this report on problems relating

specifically to superconducting magnetic spectrometers. In particular, we have spent almost all of the support provided for this contract in investigating new cryostat parameters appropriate to the shuttle weight and duration constraints. We have found that the size and weight of the cryostat, for a two-month lifetime, can be substantially reduced from that contemplated for HEAO. This conclusion is quite authoritative since it came from the same computer model which correctly predicted the thermal performance of the HEAO model cryostat, updated to include new thermal conductivity data and the appropriate shuttle sortie parameters. Moreover, with the reduced documentation requirements contemplated for the space shuttle, a considerable cost savings relative to HEAO can be realized. Since a superconducting magnetic spectrometer has considerable magnetic fringe field, we have included a section describing methods for shielding sensitive electronic and mechanical components of other experiments, or the space shuttle itself, from the effects of the field. Experiments placed further away than the immediately neighboring pallet will see a magnetic field only slightly greater than the Earth's. Since even the neighboring pallet's components see a field of less than 100 gauss, magnetic shielding can be accomplished for practically all sensitive locations by passive, high-permeability shields. In summary, magnetic spectrometer experiments are still technically feasible and scientifically important for space flight, and the space shuttle sortie mode provides an extremely useful means of deploying such experiments.

II. Spectrometer Configuration

Figure 1 is a schematic drawing of the design for the shuttle orbiting magnetic spectrometer. A charged particle traversing the spectrometer is deflected through an angle proportional to the line integral of the magnetic field ($\int B \times dl$) and inversely proportional to its momentum per unit charge. The spectrometer consists of three major systems: (1) scintillators to define the entering particles and to measure their charges; (2) spatial detectors to measure the trajectories and thus the deflection angle; and (3) a superconducting magnet to provide the deflecting field.

In the shuttle cryostat, the magnet is integrated in such a way that it can be energized remotely in space with limited power, provide a very strong experimental magnetic field but a limited fringe field, operate in any attitude, undergo transition to a normal (non-superconducting) state non-catastrophically, and have an acceptably low net torque in the earth's field. The magnet consists of a pair of relatively large, yet compact coils connected in series and mounted inside the cryostat with one coil as near to the spatial detector array as possible. The near coil provides the field to deflect the cosmic rays. The other coil is arranged with an opposing field to cancel the dipole interactions with the earth's magnetic field, so as not to influence spacecraft guidance and attitude control, and to decrease the magnetic fringe field outside the spatial detector region, so as to minimize the effect on other experiments.

The spectrometer assembly itself occupies a cylindrical space of about 1.6 m dia x 3.8 m long and is readily skid mounted. Preliminary studies have placed the overall system weight at 1230 Kg (2700 lbs) with the following breakdown:

TABLE 2 Weight Breakdown

Subsystem	Estimated Weight (kG)	(lbs)
A. Cryostat and magnet assembly filled to 15% ullage (lift-off wt)	680	1500
B. Detector assembly including removable cover shell	180	400 (approx.)
C. Detector gas supply system	90	200 "
D. Electronics and power supplies	135	300 "
E. Skid mount assembly	135	300 "

A. Design Rationale

The spectrometer design configuration selected for the magnetic spectrometer space shuttle experiment has been motivated by the following rationale:

1. The spectrometer geometry factor is influenced primarily by the magnet/detector configuration and secondarily by the magnet's cryogenic enclosure encroachment.

2. The existing magnet/detector configuration is the result of extensive previous optimization studies performed at LBL for the HEAO-B magnetic spectrometer experiment (ref. 1).

3. A laboratory-like cryogenic enclosure is required for the superconducting magnets whether they be cooled by a simple passive cryostat or a more complex cryostat/mechanical refrigerator system.

4. There are significantly fewer interfaces and failure modes for a simple subcritical cryostat magnet enclosure than for a cryostat/refrigerator system.

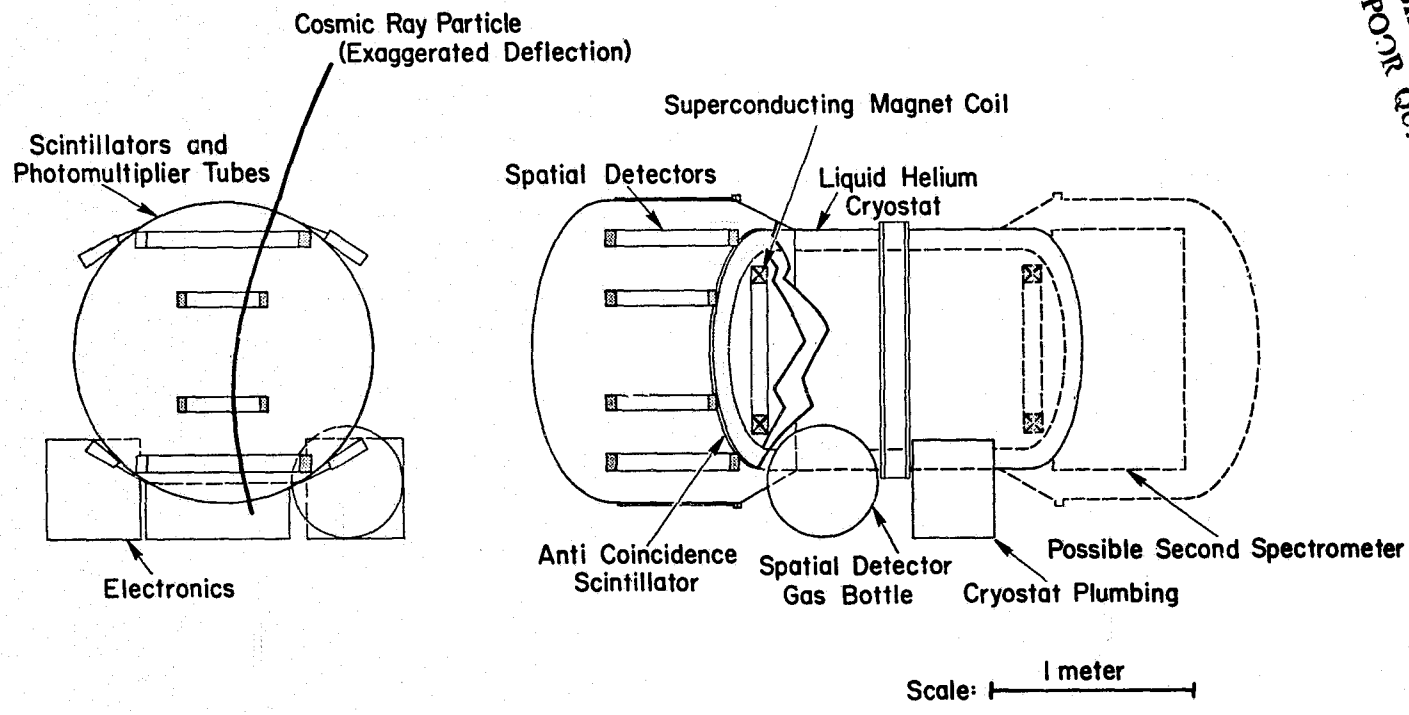

FIGURE 1. Schematic diagram of a superconducting magnetic spectrometer for Space Shuttle.

5. The effective field in the spatial detector region falls off quite rapidly with axial distance from the near coil, so it is extremely important to minimize the distance between the near coil and the inner near edge of the spatial detectors to ensure a sufficiently high $\int B \times dl$ to accurately measure the higher energy events. A smaller thickness, however, decreases the effectiveness of the cryostat thermal protection system and reduces cryostat and magnet lifetimes, so a compromise is necessary.

6. The selected cryostat design is generically identical to the design proposed for HEAO-B which has been thermally modeled and lab tested. The required thermal performance has been demonstrated. Because weight is not the serious constraint it was for HEAO, inner and outer shells can be made thicker to reduce design and test costs. The shorter lifetime, however, permits a smaller overall cryostat.

7. The superconducting magnet system design is identical to that developed for HEAO-B. Its required performance and reliability have been demonstrated.

B. Baseline Cryostat Design

The low temperature environment required for the relatively large superconducting magnets for a space shuttle experiment is provided by a compact subcritical helium cryostat. The cryostat thermal protection system consists of a laboratory-like hard-vacuum outer shell, multilayer insulation, two 0.8 mm thick aluminum vapor-cooled shields, and an inner shell. The innermost vapor-cooled shield acts as a boiler, or external thermodynamic phase separator in a liquid expulsion mode. The cryostat inner shell is provided with a stiff array of fiberglass-epoxy band

tension supports connected between a central outer shell girth ring and four uniformly distributed attach points at each end of the helium pressure vessel. These supports are mechanically and thermally connected to the two vapor-cooled shields to provide the necessary stiffness and intercept some of the heat conduction which would otherwise flow directly to the inner shell.

The pressure vessel is to be insulated with one layer of low-emittance foil, whereas the inner and outer vapor-cooled shields are to be wrapped with about 9 layers and 27 layers, respectively, of 0.006 mm thick double-aluminized Mylar with a 0.1 mm-thick Dacron net spacer applied to a layer density of about 26 layers/cm maximum. The thermal protection system annulus is 11.4 cm everywhere except at the spatial detector ends where the coils are mounted. Here the minimum annulus dimension is 5.7 cm on the axis between the torrispherical heads (which approximate 2.5/1 ellipsoids) to maximize the detector geometry factor.

The cryostat has a 2.2 m-long stainless steel fill line, a 3.2 m-long fill-vent line, and a 25 m-long shield heat exchanger line. The shield line starts at a tee, approximately 1.0 m from the pressure vessel, in the fill-vent line on the boiler shield, is wrapped in serpentine fashion over the shields, and terminates at the tank pressure regulator outside the outer shell.

All instrumentation to the cryostat pressure vessel is contained in either the fill line or the fill-vent line, thus eliminating the need for cold-vacuum-tight electrical feedthroughs.

This design is generically identical to the design proposed previously (ref. 1) for the magnetic spectrometer experiment on HEAO-B except the cryostat is smaller and lighter. The capability of meeting the stringent

HEAO cryostat design requirements were demonstrated by the HEAO Thermal Model Cryostat (TMC) which was built by AiResearch. The TMC has recently undergone a series of tests at the Johnson Space Center (JSC) in Houston. In these tests, the TMC met the original HEAO cryostat's year lifetime thermal performance goal with a measured steady state vapor expulsion mode mass flow rate of .08 lb/hr. Limited testing in the inverted mode verified the stability and effectiveness of the boiler shield concept for liquid expulsion. In addition, the superconducting magnets have undergone charging tests by JSC personnel at up to 110 amps (HEAO magnet design current) with no measured coil degradation over previous operational tests performed by LBL (ref. 3) prior to shipping the coil to AiResearch for integration into the TMC.

We plan to exploit the extensive design experience developed over the past 5 years for the space shuttle experiment by utilizing as much of the proven HEAO cryostat in-house and contractor developed technology as possible. This overall system design philosophy is expected to produce the highest reliability shuttle experiment at the lowest possible cost. Details of the Baseline cryostat conceptual design are listed in Table 3. Table 4 compares this baseline design with that of HEAO.

TABLE 3 Cryostat Baseline Design Details (see Figure 1)

Outer shell cylinder diameter	48.0 in
Outer shell overall length	73.5 in
Outer shell weight (alum. alloy) including girth ring	263 lb
Pressure vessel outer diameter	38.75 in
Pressure vessel overall length	67.0 in
Pressure vessel weight (alum. alloy)	184 lb
Outer vapor cooled shield weight	35 lb
Inner vapor cooled shield (boiler) wt	32 lb
Multilayer insulation wt	13.8 lb
Liquid helium wt at lift off (15% ullage)	262 lb
Usable helium weight (assumes 40 lb charging loss)	180 lb
Superconducting magnet weight (2 coils)	700 lb
Total cryostat weight at lift off not including mount (includes plumbing, internal supports, etc.)	1503 lb
Cryostat liquid expulsion mass flow rate	0.132 lb/hr
Cryostat liquid expulsion liftime	1367 hrs
Cryostat vapor expulsion lifetime	1671 hrs
Mission requirement (time on orbit, assumed)	720 hrs (30 days)

The cryostat's principal mounting support attaches to the girth ring which lies midway between the two superconducting coils. This girth ring also provides most of the access ports for filling, emptying, and monitoring the cryostat, as well as the electrical connection for energizing the

magnets and monitoring the cryostat vital functions. A supporting bracket will connect the cryostat to the pallet mounting points, and unless some particularly heavy additional instruments are incorporated into the final shuttle spectrometer experiment, these supports are likely to provide the mounting for the entire experiment. In figure 1 we have reserved a location for cryogenic support equipment in flight, and this is a suitable location for much of the apparatus, but connecting tubes and electronic interconnections are likely to be routed around the cryostat girth ring.

TABLE 4 Comparison of Shuttle Cryostat with Previously Proposed HEAO-B Cryostat (Ref. 1)

PARAMETER	UNITS	SHUTTLE	HEAO-B
Total wt. @ lift off	lbs (KG)	1503 (682.)	2892.(1312.)
Dry wt.	lbs (KG)	1242 (563.)	1942.(881.)
Usable He wt.	lbs (KG)	180 (82.) (15% ullage)	800.(363.) (5% ullage)
Magnet assembly wt. (Inc. internal supports)	lbs (KG)	700(318.)	700.(318.)
Liquid expulsion lifetime	(DAYS)	57.0	365 (Inc. 81 days rotating)
Vapor expulsion lifetime	(DAYS)	69.6	468
Mission duration (assumed)	(DAYS)	30	365

C. Cryostat Design Analysis

The conceptual design of the shuttle cryostat was performed using the LBL developed, vapor cooled shield cryostat design program, HELNO (ref. 5). This code was developed from the Ball Brothers Corporation one-dimensional computer Code, HEL-2.

The HELNO code was used in 1971/72 for the conceptual design of the HEAO Thermal Model Cryostat (TMC). The ability to achieve the stringent one-year helium lifetime requirements of the TMC was demonstrated in 1977 through operational tests performed at the Johnson Space Center (JSC) in Houston.

The HELNO code has also been used to calculate the vent rate on conventional vapor cooled shielded, 500ℓ Laboratory dewars (unpublished documentation available) with good agreement to measured rates. HELNO was also used to *predict* that the 6 month duration (design goal), two vapor cooled shielded Oxygen Thermal Test Article (OTTA) which was built by the Beech Corporation for NASA JSC would have a helium lifetime in excess of one year. This was subsequently verified at Beech with add-on funding from JSC to perform the test.

1) Multilayer Insulation Heat Flux

The HELNO code incorporates the MLI heat flux correlations developed by LMSC (Sunnyvale) under contract to NASA LRC from guarded flat plate calorimeter tests. Ball park, as applied "degradation factors" were determined empirically for the DAM-silk net system used on the HEAO TMC through liquid nitrogen tests performed by AiResearch (Torrance) on an existing, 18 inch diameter spherical cryostat. These degradation factors are currently being assumed by AiResearch (which built the TMC) to correlate test

results on the TMC. These same factors have been assumed for the conceptual shuttle cryostat design described herein.

2) Support Heat Leak and Structural Design

The shuttle tank annulus support heat leak was computed using a fiberglass-epoxy thermal conductivity function curve fit to values measured by Hust of NBS in 1977 on specimen cut from spare HEAO TMC support bands.

The thermal conductivity of these fabricated bands can be expressed approximately by:

$$K(T) = -.01533 + .02644T - 0.7324 \times 10^{-3} T^2 + 0.6825 \times 10^{-5} T^3 - 0.1609 \times 10^{-7} T^4 \ (w/m°K)$$

for: $4.0 \leq T(°K) \leq 280.$

The shuttle cryostat inner vessel support configuration is virtually the same as that proposed by AiResearch for HEAO-B and used on the TMC. This system consists of 16 each fiberglass-epoxy band supports between the central outer shell girth ring and the ends of the cylindrical portion of the helium pressure vessel. The support area-to-length ratio has been established to provide an inner tank axial natural frequency of 30 Hz (based on the inner tank filled to 15% ullage) to keep launch load factors at a safe level. The lateral natural frequency has not been calculated, but is estimated to be above about 18-20 Hz.

3) Helium Pressure Vessel Design Rating

The structural integrity of the shuttle cryostat helium pressure vessel, as for any cryogenic container, is extremely important from the standpoint of safety. A simplified schematic of the HEAO cryostat helium system as it was perceived in 1972 is shown in reference 5, figure 4. The

shuttle cryostat design would be quite similar except the inner tank internal rupture disc shown would not exist. This would be outside the tank in the plumbing for the fill vent line and fill lines.

It should be emphasized that all portions of the cryogenic system which could be valved-off or ice plugged with entrapped gas or liquid will be equipped with relief valves. In addition to helium system primary protection, the vacuum envelope will be equipped with a large, low impedance relief valve and parallel rupture disc to vent helium to outside of the vehicle in the very unlikely event of inner tank rupture.

The inner tank is designed with sufficient margin of safety to contain anticipated operational pressure rise, and is further protected with relief valves and rupture discs which vent outside the vehicle through thrust nulling tees so as not to upset vehicle attitude control.

Overpressures in the helium system beyond the normal, one atmosphere, operating pressure differential can result from either the sudden loss of vacuum (which could be quickly restored on orbit) or a sudden transition of the coils from the superconducting to the normal resistance state.

The inner helium vessel will be fabricated from 2219 aluminum alloy into two equal half shells and heat treated to the T6 condition for general lightness of weight. The heat treated material ultimate strength is expected to be well in excess of about 35,000 psi. However, the short, central cylindrical closure region will be locally annealed due to close-out welding. This section will be fabricated from thicker plate, roughly twice the thickness of the rest of the cylinder. The inner tank design thickness is based on a maximum material stress of 24,000 psi (for the T6 part) at a maximum internal pressure of 160 psi.

After final closure, 100% x-ray inspection, and preliminary leak

testing, the inner tank will be proof tested in a suitable test area with room temperature nitrogen gas at a pressure differential of 144 psi.

4) Maximum Pressure Rise with a Magnet Transition

The maximum pressure rise due to a magnet transition in the shuttle tank is higher than that anticipated in the HEAO-B design because of the smaller tank helium volume. The shuttle tank ullage and design pressure rating have been increased to mitigate much of the increase.

The maximum tank pressure rise is a function of the tank volume, ullage, and vent impedance, and the coil current, inductance, mass, and equivalent specific heat. Exact calculations of the transition process rise are extremely complicated because of the many assumptions that must be made regarding time and position dependent fluid state, local heat transfer, and energy sharing between the coil, coil form, and the stored fluid.

These complexities were anticipated when the TMC was built and transition testing was included in the overall operational tests conducted at JSC, Houston. However, testing of the TMC was concluded after thermal performance tests and magnet charging tests were completed because of limited funds. The single coil has thus not been transitioned in the Thermal Model Cryostat. It was discharged at a controlled rate through external diodes.

Because of the foregoing uncertainties, we have adopted a conservative approach at this phase of the conceptual design and have based the cryostat internal pressure rating on worst case transition pressure rise plus a small margin of safety. We have increased the inner shell burst pressure, increased the minimum ullage to 15% and provided the required annulus insulation to achieve a reasonable mission life margin of safety.

The worst case transition pressure rise is easily calculated assuming

a constant volume (zero venting) heat addition process while ignoring sensible energy changes in the 700 lb coils and coil forms.

Assume the inner tank volume exclusive of the coils and coil forms is $V_T = 38.74\ ft^3$ ($1.097\ m^3$). The total weight of helium liquid plus vapor at 15% ullage and 1.0 atmosphere (4.22°K) is $W_T = 262.21$ lbs (118.9 Kg).

The initial fluid quality is:

$$X_i = \frac{\frac{V_T}{W_T} - U_L}{U_V - U_L} = \frac{\frac{1.097}{.1189} - 8.001}{59.21 - 8.001} = \underline{.02385}\ \text{Kg Vapor/Kg liquid}$$

The initial fluid enthalpy and specific volume are then:

$$h_i = h_{iL} + X_i\ (h_{iV} - h_{iL}) = 9.711 + .02385\ (30.13 - 9.711)$$

$$= 10.198\ \text{j/gm} = \underline{2.437}\ \text{cal/gm}$$

$$V_i = U_{iL} + X_i\ (U_{iV} - U_{iL}) = 8.001 + .02385\ (59.21 - 8.001) =$$

$$\underline{9.222}\ \text{cc/gm}$$

The stored energy in the magnetic field of each coil at the design current (110 amps) is 0.725 Mj. Assuming none of this energy is absorbed by the 700 lbs of SCM during a transition, the maximum enthalpy change of the tank fluid becomes:

$$\Delta h_{if} = \frac{2(0.725 \times 10^6\ \text{j})}{(.1189 \times 10^6\ \text{gm})} = 12.191\ \text{j/gm} = \underline{2.914}\ \text{cal/gm}$$

The final fluid enthalpy is therefore:

$$h_f = h_i + \Delta h_{if} = 2.437 + 2.914 = \underline{5.351}\ \text{cal/gm}$$

Following a constant volume line on a temperature-enthalpy diagram for helium from initial state at $P_i = 1.0$ atm, $h_i = 2.437$ cal/gm to the final state at $h_f = 5.351$ cal/gm we get $P_f \approx 7.1$ atm = $\underline{104.3}$ psia.

With the helium vessel proof tested to 144 psi at room temperature, the safety factor against rupture is at least:

$$S.F._m = \frac{144}{104.3} = \underline{\underline{1.38}}$$

Had sensible energy changes in the coil been "incorporated" in the forgoing calculation, the maximum pressure rise would have been lower. Earlier transition tests of these coils in a well vented laboratory dewar bear this out - for a transition from 110 amps, we typically find the coil tempertature rises to about 70-80°K for several tens of seconds before finally cooling to the bath temperature.

The forgoing 1.38 rupture safety margin will also be somewhat higher due to increased vessel strength at cryogenic temperatures, however we haven't included this fact here.

5) Venting and Relief Provisions

The shuttle cryogenic helium tank will normally vent through an absolute pressure regulator attached at the warm end of the vapor cooled shield line. This is a relatively high impedance line. This regulator will be set at between 15.0 and 16.0 psia.

The two low impedance tank lines (the fill line and the fill-vent line) will be externally coupled and equipped with a safety relief valve and parallel rupture disc. This line will then be routed to the outside of the vehicle terminating in a thrust nulling tee.

The setting of this latter relief valve is to be determined.

D. Magnet Design

Table 5 is a relatively complete description of each of the two coils proposed for the shuttle experiment. These coils are identical to the one built and tested for the HEAO-B thermal model cryostat (Ref. 1).

Several key features can be noted in the coil described in Table 5. They are mainly dictated by requirements of the application, such as: (1) high field at the wire and high current density; (2) moderate size, weight, and stored energy; and (3) relatively low current. The coils are also rugged and reliable.

If a small region in these high-current-density coils undergoes transition to normal conductivity because of loss of cooling, excessive currents, wire movements, etc., the wire will heat very rapidly. Unless the current is quickly reduced, local overheating can occur. These coils have very high inductance because of the requirement for low current. This makes rapid coil discharge to an external load, such as a series resistor, impossible because of the high voltages required. Therefore, in case of accidental discharge, most of the magnetic energy must be dissipated as Joule heating within the coil windings. It is important to design the coil so that any local "hot-spot" or normal region will cause the entire coil to become normal in a period of time which is short enough to prevent local overheating. This will result in most of the magnetic energy being dissipated nearly uniformly throughout the windings. The spread of a normal region throughout a coil is a complex process to analyze, because it involves heat conduction across layers, along the wire, and turn-to-turn heat transfer by helium in the windings (which has become heated, and, therefore, pressurized), and by Joule heating caused by short-circuit currents which

may be transmitted between turns during rapid discharge. The latter effect is due to the use of a "semiconducting" material for turn-turn insulation. The details of the transition process in the coils are presently not understood. However, measurements of discharge characteristics of previous similar coils show that at design current, these coils become normal in less than about 1 sec, and that the energy does dissipate nearly uniformly throughout the windings.

This design philosophy results in a system which is "passively" safe and does not need an active protection system. If these coils were constructed to be more stable, for example, by using a better cooling geometry, the rate of "going-normal" might be reduced to a degree which would cause the coil to be damaged on discharge. Thus, it is desireable to have the coils just stable enough to permit predictable and reliable charging and operation, but unstable to large disturbances.

The HEAO-B coil has been made persistent several times at LBL and JSC to currents up to 110 A but has not yet been driven normal; instead, it was discharged through external diodes.

Because liquid helium is diamagnetic (see ref. 2), it is expelled from the immediate region of the coil windings in zero gravity. This may reduce the potential stability of the coil to local heating and hence transitions because the heat conductivity of helium vapor is less than that of the liquid. However, the conductivity of the vapor is probably sufficient, and is perhaps better than that achieved with a potted coil. Nevertheless, additional investigation of alternative cooling/protection schemes such as potting is advisable before finalizing the coil design. (Moreover, the cryostat design affords the required lifetime even with liquid expulsion from the vent tube, so diamagnetism does not significantly affect the placement of the vent tube.)

TABLE 5 HEAO-B Coil Parameters

Outer diameter D_o, cm	84.5
Inner diameter D_i, cm	68.2
Length L, cm	9.52
Total Magnet weight, kg	150
Total ampere-turns	1.13×10^6 *
Apparent current density J_a, A/cm^2	14,600
Max. operational current I_m, amps	110 **
Design current I_o, A	120
Max. design field at wire H_m, kG	70
Stored energy MJ (per coil)	0.725 *
Measured inductance L, Henries	119.5
Mean useful magnetic field integral ($\int B \times dl$), kG-m	5.0
Superconductor type	Nb-Ti, Cu-clad
Number of filaments	180
Copper-to-superconductor ratio	1.8/1
Wire insulation (turn-to-turn)	Cu oxide (Ebanol C)
Layer-to-Layer insulation, 0.2 mm Glass cloth	2 layers
Winding tension, kg	3.5 (approx)
Splice length, turns	0.94
Total turns	10,285 §

Coil Region	Inner	Middle	Outer
Turns distribution	880	947	8458 §
Layer distribution	8	8	70 §
Wire diameter, mm	0.890	0.812	0.762
Twists per cm	1.2	1.2	1.2

* Based on existing coil (86 layers) at 110 A current.

** Maximum operational current not yet determined (120A est.); tested to 110 A.

§ Original design called for 80 layers in outer region.

E. PERSISTENCY SWITCH DESIGN

The persistency switch for the shuttle magnetic spectrometer will be identical to that built for the previous HEAO-B experiment. The following is a description of the switch designed for HEAO-B and built and tested in the HEAO-B thermal model cryostat (Ref. 2).

Rather than supply current continuously to the magnet from an external source, since power is limited in satellites, the choice was made to complete the superconducting circuit inside the cryostat and keep the magnet charged with a persistent current. However, to charge or discharge the magnet it is necessary to be able to open and close the superconducting circuit. This is accomplished with the use of a section of superconductor called the "persistency switch," which can be switched from its superconducting to its normal-resistance state by means of a heater. This switch is mounted in parallel with the coil in the coil-charge lead circuit.

Desirable characteristics of the persistency switch for these high-inductance coils are: (1) relatively high resistance in the normal state in order to minimize current in the switch during charging of the coil (about 10 V maximum is required to charge these high-inductance coils in times of 1 hr or more); and (2) low switch inductance in order to minimize energy stored in the switch, stray field in the switch, and switching time. A copper-nickel matrix composite wire has been chosen to provide the high normal-state resistance with a one-to-one matrix-to-superconductor ratio for electrical stability. Half of the superconductor turns are reverse-wound to keep the switch inductance low. The persistency switch, which is always connected across the coil terminals, is designed to carry the coil current during a discharge without overheating, assuming that it will be driven normal at the same time as the coil.

The switch is very stable. It is well insulated thermally. When the applied voltage is above 0.25 V, enough self-heating occurs to prevent recooling to superconducting temperatures. Since the coil will be charged in the range of 1 to 6 V, this means the heater is not needed during charging, except to initially heat the switch until it becomes normal.

These persistency switches have been tested repeated to 150 A and occasionally to 200 A at zero field. The switch and magnet we have flown in our balloon experiments have been kept persistent several times at currents over 110 A for a couple of weeks at a time with no measureable current loss (less than 1%).

It is important that there be no appreciable current loss due to either the switch or magnet, for two reasons. First, it is desirable to maintain the high magnetic field. Second, since the satellite coils would each contain about .73 MJ, a significant decay rate would generate too much heat within the cryostat. A maximum loss rate of the magnetic field energy of about 10% per year is tolerable for maintaining required experimental accuracy. This would increase the cryostat heat input by about 1.4%.

The persistency switch is a 10.2 cm-long by 6.35 cm OD solenoid of superconducting wire interwound with two separate Manganin wire heater coils. One heater is for redundancy. The coil form is a 4.45 cm-OD Micarta tube with 0.32 cm-thick walls.

The superconductor is 5.09 turns of Kryoconductor No. 32, which is a 0.76 cm-diameter Nb-Ti multicore superconducting wire embedded in a Cu-Ni matrix with matrix-to-superconductor ratio of one-to-one. This wire has 500 Nb-Ti filaments, 0.39 twist per centimeter, and is insulated with Formvar. Two layers of superconductor are wound in a clockwise direction and two layers in a counterclockwise direction. Each layer of wire is insulated with two

layers of 0.13 mm-thick glass cloth. This construction allows enough cooling when immersed in liquid helium to be stable. Yet, only a small heat input is required to keep the superconductor above the transition temperature of about 9° K.

Each side of the switch is connected to the coil by a single strand of the Kryoconductor No. 32 plus two parallel strands of Kryoconductor No. 157 (Nb-Ti composite with a copper-to-superconductor ratio of 1.8 to 1,180 filaments with 1.2 twists per centimeter, and copper oxide insulation) soldered together with indium in a compact three-wire bundle. Construction details and measured characteristics of the completed HEAO-B switch are listed in Ref. 2.

F. Current Leads

The magnetic spectrometer shuttle experiment anticipates the use of magnet current leads similar to those used on the HEAO magnet. However, with the higher anticipated cryostat vent rate (lead coolant) the leads have a slightly larger area-to-length ratio. The budgeted zero current lead heat leak has been conservatively increased to 0.2 watts.

A very important reason for using small-diameter superconducting wire in these coils is to minimize the coil current and therefore to minimize the steady-state heat leak due to the magnet charging leads. While using larger wire or ribbon could reduce winding costs, the charge leads would have to be larger to carry the increased current necessary to produce the same magnetic field. The leads are not disconnected after charging, since complete thermal disconnection is much more complicated an operation than electrical disconnection, and high system reliability and magnet protection are desired. Also, 100-A power supplies are more feasible than significantly higher current power supplies in satellites.

There are four insulated charge leads (two are spares) about 3.2 m in length which run down the inside of the fill-vent line to the pressure vessel. The innermost 1.0 m of the leads is cooled by steady-state boiloff from the cryostat before it is routed to the vapor-cooled shields. The lead cross section tapers down in three steps from #16 AWG copper (1.3 m long) at the warm end, #20 AWG high-purity copper (1.3 m) in the middle, to the final section of 0.8 mm-diameter superconducting wire of 1.8/1 twisted Nb-Ti multicore, about 0.6 m long.

A reasonable charging profile for the magnet assumes full current can be developed in about four hours. The maximum coolant mass flow rate required to prevent lead thermal instability at 15% above the design current is less

than 3.0 Kg/hr (6.6 lb/hr). The baseline design has 40 lb of liquid helium budgeted for magnet charging.

This flow can be established by several methods, including: controlling the discharge pressure of the vent tube, or controlling the vapor pressure of the helium by using the auxiliary heater in combination with other heat sources such as eddy-current heating. Details of the HEAO-B charge leads may be found in Ref. 3.

III. MAGNETIC SHIELDING GUIDE

The magnetic spectrometer experiment has a magnetic fringe field around it. The most important impact of this fringe field, the dipole interaction with the earth's magnetic field, is removed by placing two coils in opposition within the cryostat. The second coil can also support a second experiment at the other end of the cryostat. In spite of the first-order cancellation, large fringe magnetic fields still exist near the experiment. We recognize that the optimum situation for mounting experiments within space shuttle would be that all payload modules could be placed anywhere within the shuttle volume without consideration of their interaction upon one another. We feel, however, that this stringent condition not only might preclude flying a magnetic spectrometer on the shuttle, but is also entirely unnecessary. In many cases, protection against magnetic fields would consist simply of a proper placement of experiments within the space shuttle to put those which are most sensitive farthest removed from the spectrometer. If the spectrometer were situated in the rear-most pallet in the shuttle, the immediately neighboring pallet would experience fringe fields between 2 and 100 gauss, and the other three pallets would see little more than the ambient earth's field (an average of 2 gauss for the next-to-neighboring pallet). Experiments on these three pallets would presumably require no additional shielding. Even if it were critical to place sensitive experiments on the nearest pallet, the magnetic fields are not so large as to require substantial shielding modifications. The following sections present the design criteria that would apply in this case. If a neighboring experiment were shielded using these criteria, it would be necessary to check that the shielding was effective in a pre-flight test with the two experiments located relative to each other as they would be in flight. We would like to emphasize again,

however, that proper deployment of experiments within the space shuttle bay will almost certainly minimize and perhaps eliminate any need for pre-flight shielding preparations.

A. Requirements for Magnetic Shielding

Devices such as photomultiplier tubes must be shielded so they operate in magnetic fields of less than a gauss. Less stringent requirements exist for ferrite cores, relays, solenoids, and motors. Figures 2 and 3 show the intensity and direction of the magnetic field around the proposed pair of magnetic spectrometer coils. The fringe field is undoubtedly large enough to require shielding for some neighboring experiments. The field falls with distance r roughly as r^{-3}. Most shielding requirements can probably be met with simple application of high-permeability shields. Above about 100 gauss, however, additional shielding is necessary. This guide describes rules of thumb for designing the total shielding package, and discusses the impact such shields might have on experiment design.

B. Design Basics

The function of a magnetic shield is to "draw in" field lines and force them to transit the shield inside the shield material, thereby reducing the magnetic field seen inside the shielded region. Only so many lines can be drawn in before the shield becomes "saturated", producing the maximum field B_s inside that material (typically 10 to 20 kilogauss for soft iron). A shield must therefore be designed thick enough to have an internal field well below this saturated field, since otherwise the shield becomes ineffective: it merely reduces the field seen inside by a constant amount. On the other hand, a shield too thick, or one whose permeability is too low, adds unnecessary weight and increases mechanical stresses. What factors govern the

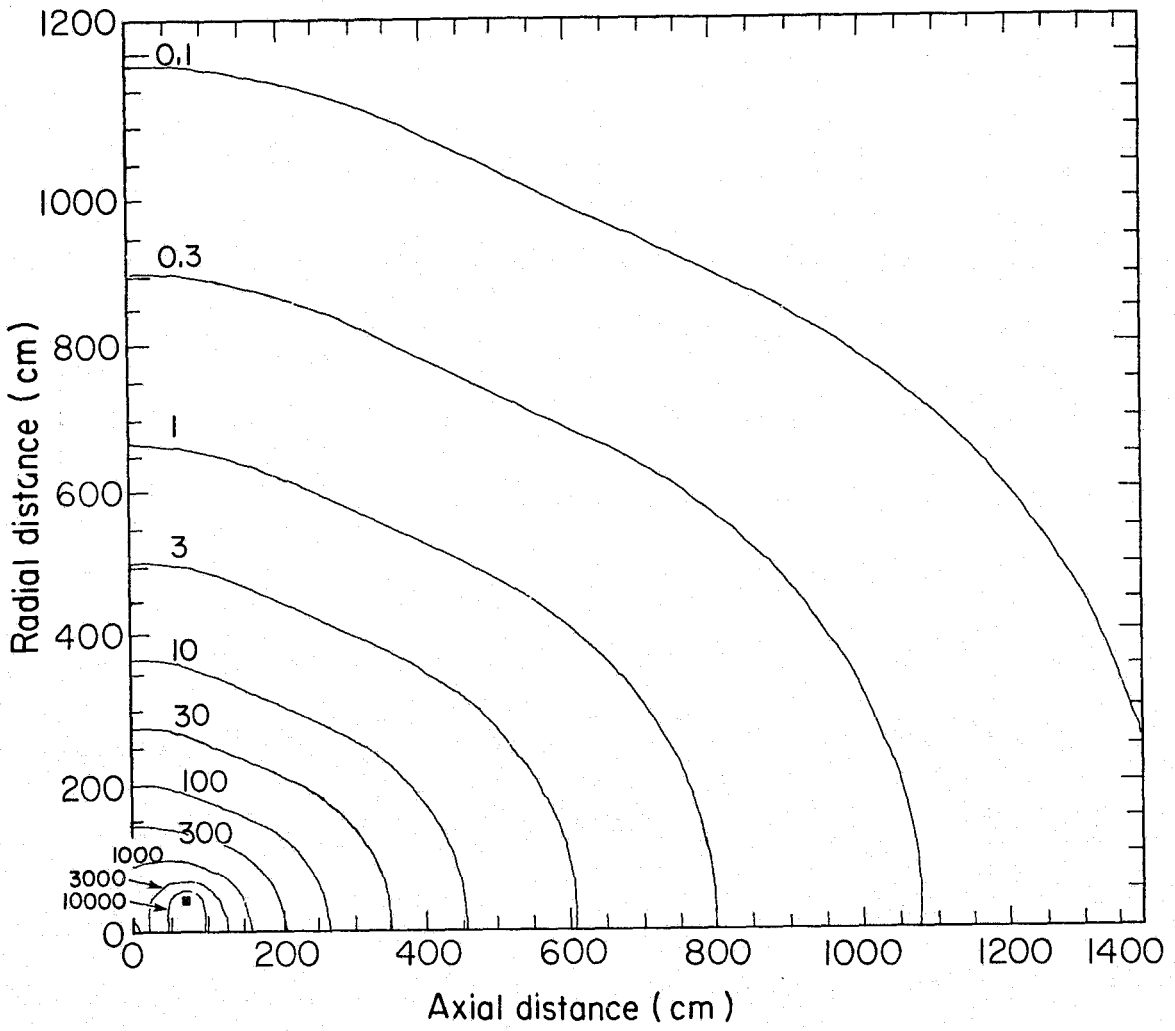

FIGURE 2. A plot of magnetic field strength as a function of position.

The field strength curves are labelled in units of Gauss.

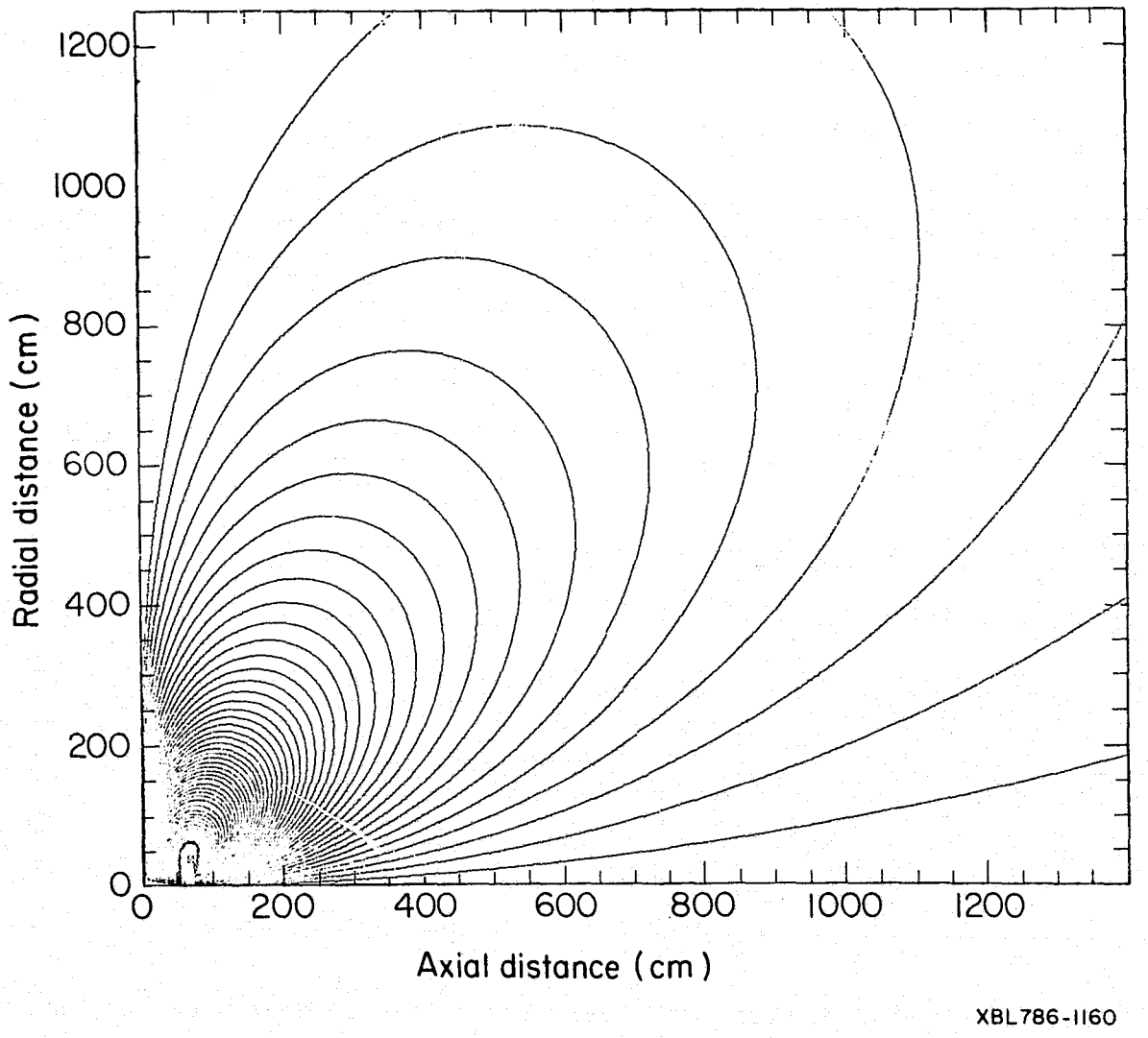

FIGURE 3. A plot of magnetic field direction as a function of position.

optimum design? Consider a hollow cylindrical shield with inner radius b, outer radius a, thickness t = a-b, permeability μ, and infinite length in a fixed uniform magnetic field B_o in air or vacuum (unit permeability). The field seen inside will be smaller than the external field by the factor (cf. J.A. Stratton, Electromagnetic Theory, 1941, p. 265)

$$G = 1 - [1 - (b/a)^2]/[\mu + 1)^2/(\mu - 1)^2 - (b/a)^2]$$

$$\approx 1/[1 + (t/2b)(\mu - 1)^2/\mu]$$

$$\approx 1/(1 + \mu t/2b)$$

where the second step assumes t much less than b, and the last step adds $\mu >> 1$. Thus the attenuation of a shield is given approximately by $(\mu t/2b)$. To avoid saturation, however, the shield must have $(2b/t)\ B_o << B_s$; this relation arises because a shield (placed perpendicular to the field direction) draws in field lines from its interior, as well as from the surrounding region (out to perhaps one more radius).

In designing a shield for a particular application, one first determines whether a single material can give the required field attenuation. This is done by checking whether $(2b/t)\ B_o << B_s$ (to avoid saturation) and $(2b/t)\ B_o << \mu B$ (to get the required field reduction), where B is the desired field on the axis inside the shield, B_o is the external field (assumed here to be DC and uniform), and B_s is the saturated field inside the shielding material. The diameter should obviously be minimized (subject to guideline 5 below), and the thickness should be in the range from about 0.5 to 10 mm (subject to weight or mechanical restrictions). The guidelines for high-μ materials (Mumetal, Permalloy, Co-netic, etc.) are $\mu \approx 10^5$ for $B_o = 10^2$ gauss, $\mu \approx 2.5 \times 10^5$ for $B_o = 10^3$ gauss, and $B_s \approx 7$ kilogauss (see

figure 4). The result is that a single material probably can do the job for shield diameters of 10 cm or less and $B_o \lesssim 50$ gauss. Nesting of co-axial shields is usually desired for $B_o \gtrsim 100$ gauss, because either the high-μ material will saturate before giving the required reduction, or because a lower-μ material which doesn't saturate ($\mu \sim 10^3$, $B_s \sim 20$ kG) won't give the required reduction. Nested shields are also more efficient in the sense that the combination does better than the sum of the two thicknesses because the inner shield operates in a lower field. The radial separation between shields must be more than a minimum which is dependent on shield design, but is roughly 6 mm for a 5 cm diameter shield. Additional guidelines are as follows:

1) μ is a function of frequency, and the physical mechanism providing the shielding changes at high frequencies, so the guidelines discussed here may be inappropriate for experiments having rotating equipment or other AC effects.

2) High-μ materials are somewhat shock-sensitive, and are best annealed after all mechanical operations because B_s is thereby increased $\lesssim$20%.

3) Make all shields <u>round</u> with no corners or large openings. Fields fringe out of the shield between the edges of a corner, dispersing inside the shielded region and hence increasing the field seen there. A similar effect occurs for holes, the effect being larger for higher concentrations of field lines within the shield material (i.e. for higher μ and/or thicker shields). Thus do not allow any changes in radius along the shield.

4) If possible, make all joints parallel to the heaviest flux direction.

5) Place all interior components on the shield axis, because the attenuation of a shield falls off roughly linearly with distance between the axis and the shield.

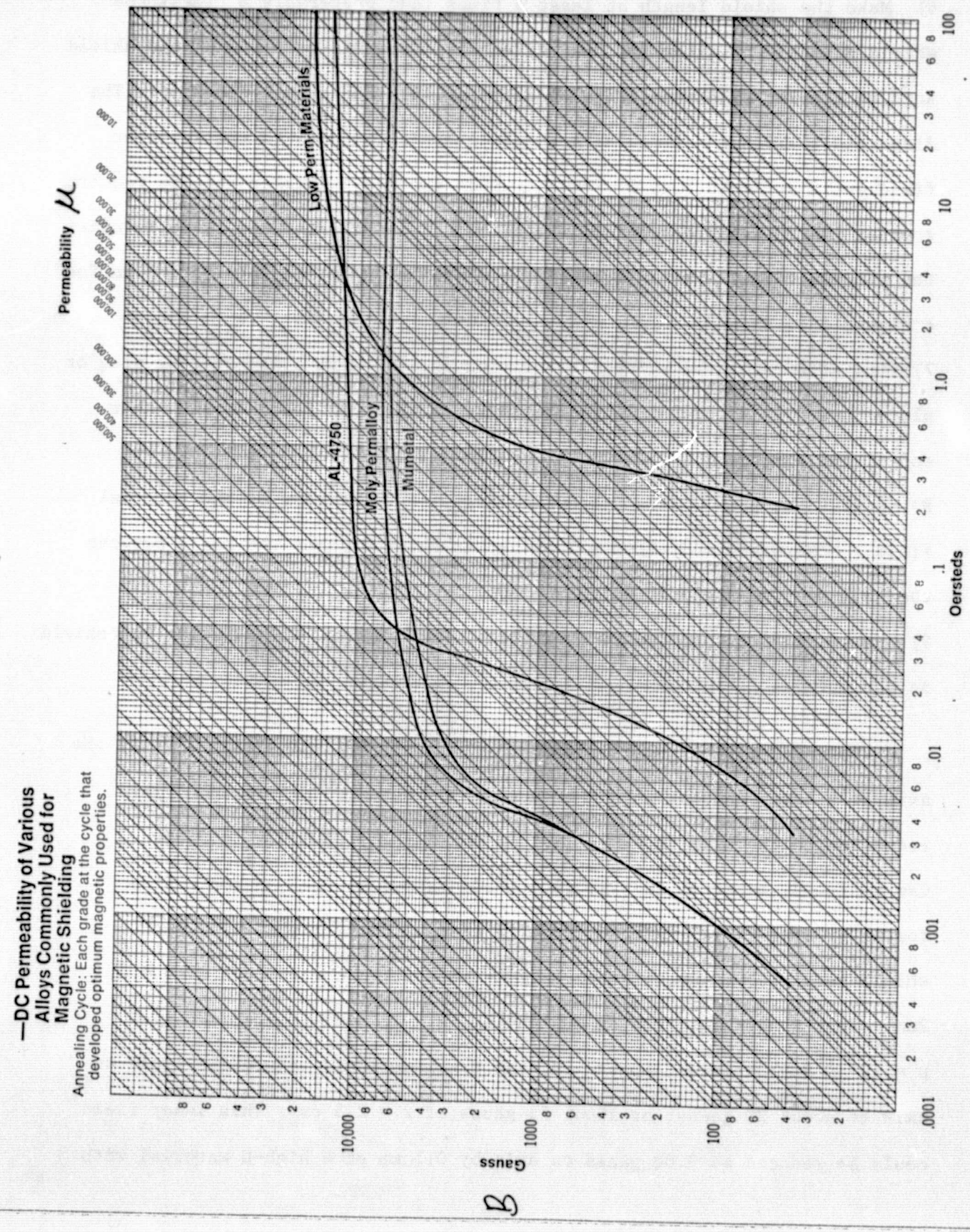

Figure 4
(from Allegheny Ludlum publication EM36-Ed-2-7M-1174 P (1974))

6) Make the shield length at least 3 times (and preferably 5 times) the shield diameter to allow for "end effects". That is, each end of the shield acts as a hole, allowing fields to disperse into the shield interior. The dispersed field for a 1-mm thick shield doesn't diminish to the interior field until at least 3 to 5 radii from the end. Thicker shields require greater length/diameter ratios. Also, if the length/diameter ratio is near the minimum there is a maximum effective thickness of the shields (~1 mm for a high-μ 5-cm shield).

7) End effects can be reduced by capping the end with a washer-type plug or plate, but such things will tend to increase the end effect at the other end of the shield.

8) Orient the shield axis perpendicular to the direction of the external field. Otherwise, end effects increase as the cosine of the angle between the axis and the field direction.

9) Never rely on formulas to judge final performance. Always test the shield in the operating field.

For example, suppose one desires 0.2 gauss or less within 1 cm of the axis of a 5-cm diameter shield with B_o = 300 gauss. The required field reduction on the axis is hence (2.5 cm / 2.5-1 cm) (300/0.2) = 2500. Can a high-μ material (μ ~ 150,000 @ 300 gauss) do the job for t of a few mm or less? - yes, because $2500(2b/t) < \mu$ for t >1 mm. Will such a shield saturate? - most likely, because saturation corresponds with t = 2mm. Thus a nested shield is desirable: e.g. a soft-iron shield with $\mu = 10^3$ @ B_o = 300 gauss, 2b = 7 cm, and t = 1 mm would reduce the field on axis to about 20 gauss, or about 75 gauss at r = 2.5 cm. This inner field could be reduced to 0.08 gauss on axis by 0.5 mm of a high-μ material with

2b = 5 cm, which yields 0.14 gauss within 1 cm of the axis.

Length restrictions become more critical in non-uniform fields because shields too long (or too thick) increase the shield mass and hence the penetration of axial fields, especially on the end with the larger field gradient. Similar comments apply for the use of end caps, or any other procedures which alter a constant-radius geometry. The fringe field from a magnetic spectrometer experiment (figure 2) is not that non-uniform, however, so these precautions need not be serious.

If many shields are used, the average field traversing the experiment will be larger, since the average permeability has been increased. One is therefore cautioned to consider the effects on nearby equipment of the use of magnetic materials to shield certain critical components.

C. Magnetic Forces on Shields

Magnetic objects placed in the non-uniform fringe field of a magnetic spectrometer experience both forces and torques due to the induced magnetization interacting with the field gradient. Typical accelerations are about g/r^3 with r in meters (g = acceleration due to gravity). Figure 5 shows a force contour plot. Thus forces are unimportant compared with gravitational forces at distances much greater than one meter, so mechanical constraints beyond these required for launch forces are not generally required. The best practice, however, is to avoid use of ferromagnetic objects in proximity to the magnet. This is of course not possible for magnetic shielding, which should therefore be tightly secured.

D. Magnetic Shielding for Spacecraft Subsystems

There are presently no magnetic restrictions for Shuttle subsystems, and Shuttle structure is primarily aluminum. Sensitivity of various subsystems to the fringe fields specified in figure 2 should nevertheless be the subject of some future study, to ascertain any shielding requirements. If the rate-gyro assemblies located in the forward equipment bay are the most sensitive critical subsystem, no shielding should be required if the spectrometer experiment is merely located in the center or rear of the experiment bay. The fringe field at the gyros would thereby be reduced to the level of the Earth's field. There are hence no known shielding requirements for Shuttle subsystems at this time.

E. Safety near Magnets

From the previous section, it should be obvious that there are potentially dangerous forces on ferromagnetic objects placed within a few meters of a strong magnet. Figure 5 shows the force contours ignoring possible saturation effects in the object being attracted. Forces at one meter are comparable with gravitational forces, and can hence be more than one person can handle, especially for large masses. Moreover, if such objects are allowed to be pulled in, they will accelerate toward the magnet and strike it at velocities comparable to those of projectiles. Any fingers which became lodged between the object and the magnet could certainly be crushed. The following safety rules should therefore be observed near any magnetic spectrometer WHILE THE MAGNET IS OPERATING:

1) No personnel uncleared by the spectrometer staff should be allowed anywhere within 5 meters of the magnet.

2) No ferromagnetic tools, screws, or other hardware can be allowed within 5 meters. Hardware items can be aluminum or non-magnetic stainless steel, for example, but not iron. The usual tools can be replaced with those made of beryllium copper alloy.

3) No person should carry watches, cameras, etc. near the magnet for fear they may not function properly thereafter. Articles so affected, however, can sometimes be returned to proper operation through de-gaussing procedures.

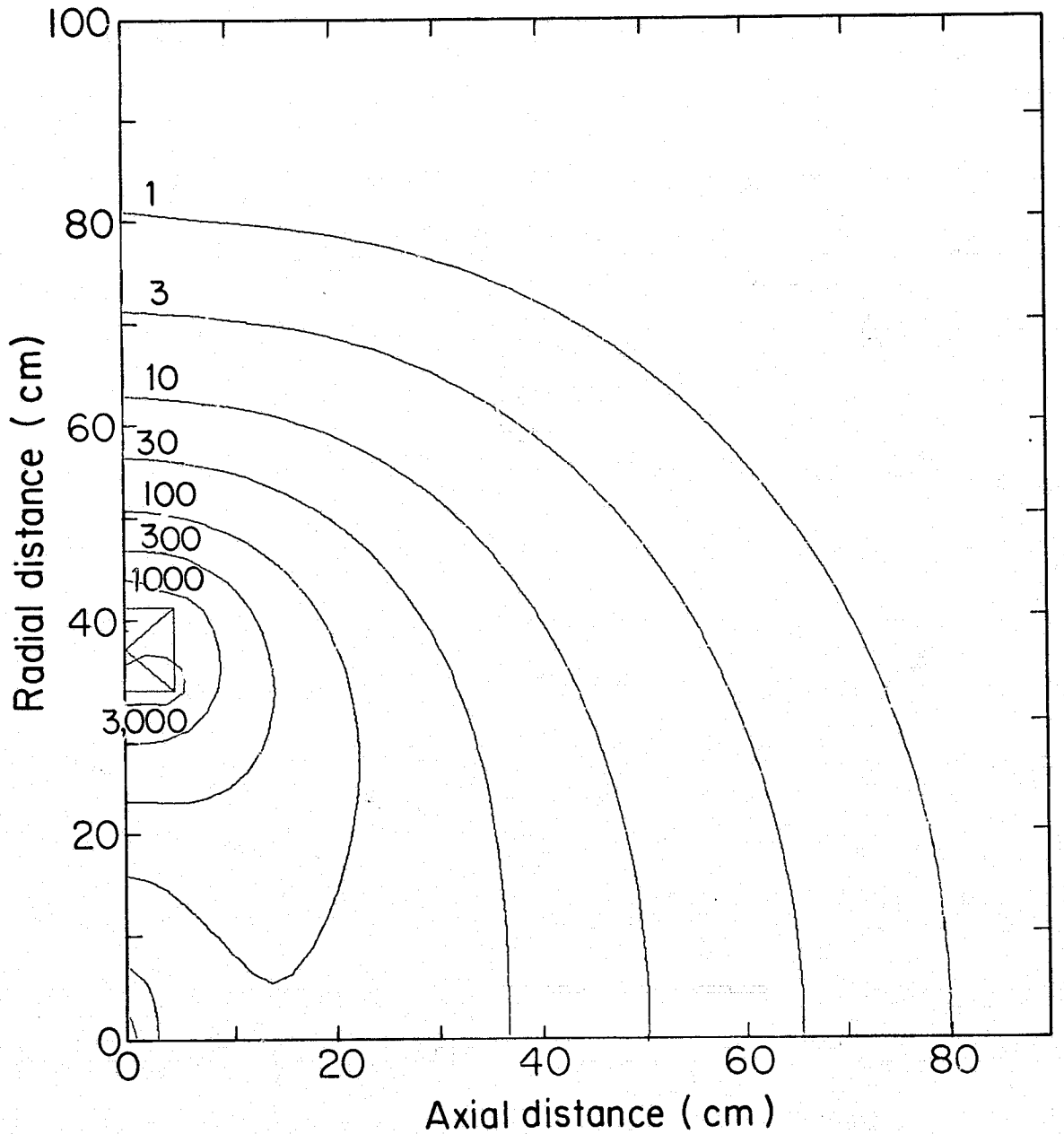

FIGURE 5. Force contours near the magnet coil. Note the scale change difference compared with figures 2 and 3. Force is in units of g (gravity at the Earth's surface), for ferromagnetic objects.

IV. Electronics

A. Spatial Detectors

The present study did not include the definition and design of the spectrometer track chambers. The construction of track chambers is a well developed technology and they have been applied extensively in high energy physics and cosmic ray physics. Thus it is unlikely that any primary development work will be needed for this system. Of course a detailed design of a specific set of track chambers which will meet the resolution, data-rate, and telemetry requirements of the spectrometer will have to be part of a full shuttle proposal.

B. Electronics Overview

The spectrometer as conceived here is a facility which could be used for many experiments. Each experiment would add a set of detectors specifically configured for the particular measurement being made. These could include for example a set of 4 or 5 scintillation trigger counters and a cerenkov counter. Although the details of the electronics for each configuration will be different, the overall scale will be comparable and many of the functions for each experiment will be identical. These detector configurations and the associated electronics will be very similar in many respects to those our group has used in many balloon flights using two generations of magnetic spectrometers. Thus to give a feeling for the scale for the electronics and telemetry requirements we present in Tables 5 and 6 and in Figure 6 the parameters and layout of the electronics used for a recent balloon flight.

An additional but minor alteration to balloon systems would have to be made to incorporate a high data rate shutdown system to turn off the data

TABLE 5

Typical Electronics Units for a Spectrometer Experiment

(from May 1977 balloon flight)

Quantity	Channel
6	Fast amplifier (X20)
12	Discriminator (50-100 mV)
2	AND/NAND 5-fold coincidence
4	Gated-OR
8	4-fold Fan Out
10	PHA with linear gate
6	Pulse shaper/converter
2	Digital scanners
10	HV Supplies for spatial detectors
14	HV PMT Supplies
2	Telemetry channels
2	Command systems
2	Housekeeping monitors
1	Power distribution center
1	Spatial detector gas control system

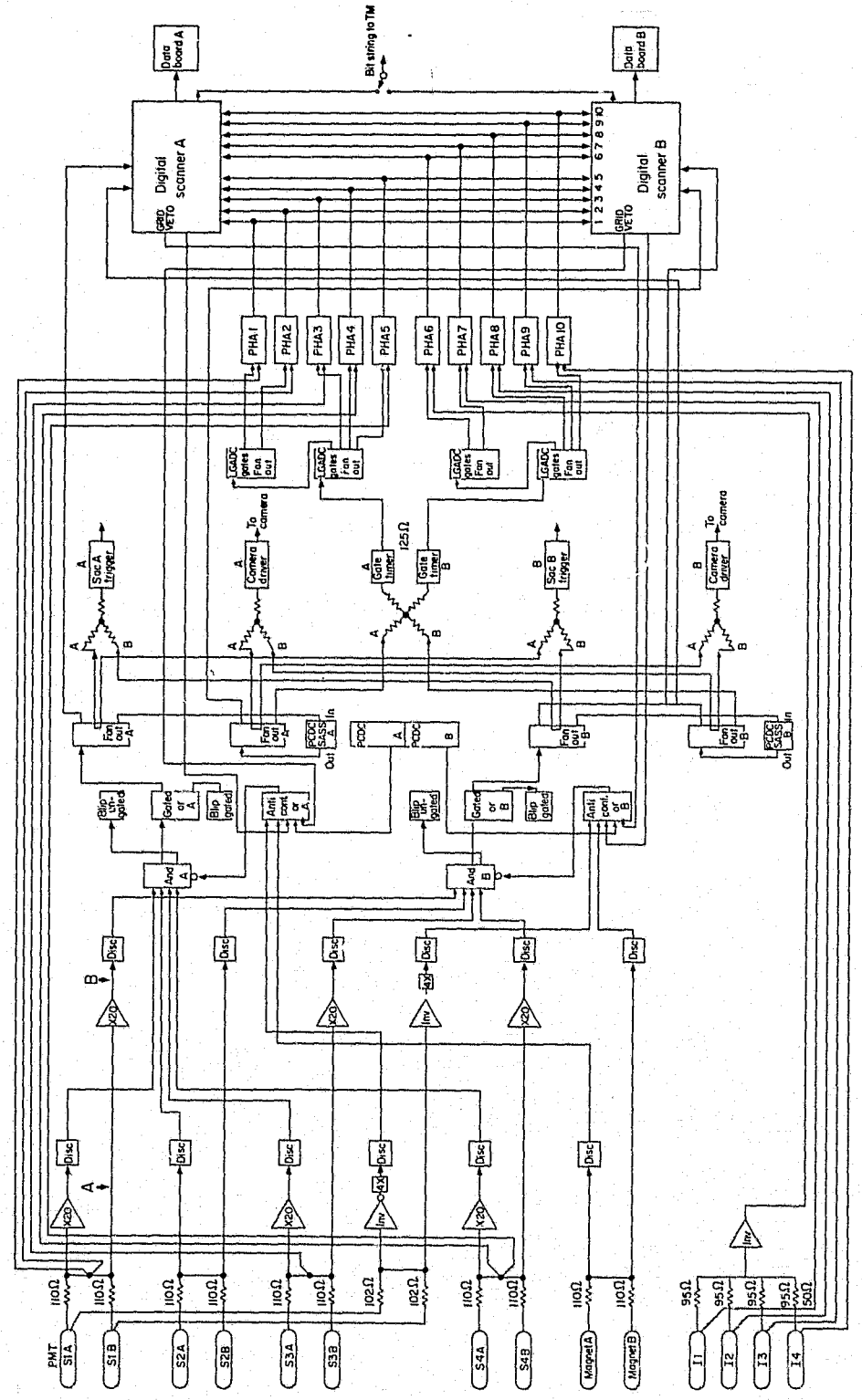

FIGURE 6. Block diagram of the electronics system used in the group's recent beryllium-isotopes measurement. The letters "A" and "B" refer to the redundant sub-systems which could be selected by real-time command to control the actual data-taking. The only non-redundant portion of this electronics is the pulse height analysis units (PHA) section, but the experimental data analysis would not have been greatly degraded by loss of either half of the PHAs.

collection when in the high intensity region of the South Atlantic Anomaly.

C. Reliability

During the group's extensive experience with magnetic spectrometers a number of operational procedures have been developed which have had significant impact of the reliability of the equipment and the success of the data collection. This reliability was achieved by (1) an electronic design philosophy which stressed redundancy, (2) by a thorough testing of electronics components (such as multiple temperature cycling), and finally (3) by a detailed and extensive checklist for preflight, flight, and post flight operations. We feel that a cost effective approach to the electronics in these experiments would be to reduce much of the usual documentation required for space flight and to increase the redundancy in the electronics and the completeness of checkout procedures.

D. Logic Circuit

In our balloon flights we have used commercially available NIM modules in the logic and analysis circuitry. We typically employed an average of 40 modules costing about $1000. each. The ability to rearrange these modules into different configurations required for different experiments has meant a considerable financial savings during the several years and many experiments. It seems likely that a great deal of commonality could exist between the various cosmic-ray experiments that will fly on the shuttle. Such commonality could result in substantial savings on electronic modules of general utility that would need space hardening. It is also possible that portions of the electronics for a completed experiment could be reassigned to a new one.

E. Bit Rate

Trigger rates in previous experiments have been typically 1 to 10 event frames per second. The information in a typical event frame is about 700 bits. In addition, housekeeping information is read out every few minutes; a housekeeping frame probably would be about the equivalent of a single event frame. If the shuttle provided a sufficient data telemetry rate, the simplest scheme would telemeter each event as it comes in, with minimal buffering. With this scheme, the data from a single flight could be as much as 10^{10} bits, although the exact amount would depend on the particular trigger criteria. Selection of the more interesting events would then take place upon the telemetered data tapes. On the other hand, if telemetry were more limited, the experiment could employ on-board data buffering, with perhaps 10K storage capability, and a selection procedure to store high-priority data preferentially. With this scheme, a total experiment would probably be more like 10^9 bits.

F. Commands

Most of the commands (for example, trigger threshold adjustments) for the experiment will be initiated from the ground, without any need for active participation by the crew. However, there will be a few critical commands that will be of active interest to the crew. Energizing the magnet may be carried out by a crew member, but even if this is controlled from the ground, the crew should be aware of the progress, because of the possibility of change in the cryogenics if there should be a magnet transition. Similarly, the crew will want to be aware of magnet discharge (although there is very small chance of transition here) and experiment power shutdown.

G. Ground Support Electronics

Because of the specialized nature of most ground support equipment, we expect this to be mostly inhouse construction. However, much of the electronics interfaces to the data tapes and real time display consoles might be quite similar from experiment to experiment, which would permit standardization and recycling.

V. Reuseability

We expect that a magnetic spectrometer will prove to be an important part of many future experiments on the space shuttle. We have already mentioned that two separate experiments may be conducted at either end of the cryostat. Although we do not feel it is proper to advertise the spectrometer-magnet-cryostat assembly as a "facility" in the same sense as would be the Large Space Telescope or the 1.2 m X-ray Telescope, it does hold the promise of being reused many times. Addition of detectors in front of and behind the spectrometer reconfigures it in whatever fashion appropriate for the experiment being attempted. Our most recent balloon gondola was reconfigured from the bare spectrometer, which was used to measure nuclei and search for antimatter, to the bremsstrahlung-identification mode for measuring electrons and positrons, and again to the isotope separation mode for our recent beryllium measurements (see Table I). A magnetic spectrometer is a versatile cosmic ray tool, and we expect that many groups will have experiments employing it.

After a space shuttle flight, the spectrometer may be flown again with only minor alterations. In this case, based on our ballooning experience, the instrument could be ready for reflight in only a few weeks, since it is necessary only to replenish the expendables and give the electronics a thorough checkout. If, on the other hand, major renovations are to be carried out, such as reconfiguration to a different experiment, the instrument might not be ready for reflight for many months.

VI. Integration and Flight

Integration starts when the instrument is shipped to the flight preparation center, where it is checked out and combined into a shuttle payload in combination with the other instruments to be flown. The technical officer for this study has informed us that the time duration for integration is expected to be about 9 months. We have brought our magnetic spectrometer experiments to the field for balloon flights eight times, and as a result have considerable experience in the length of time the instrument requires for its checkout. Typical preparation times, with a crew of typically six, are about a month. Work proceeds in parallel on the cryogenic, optical, and electronics systems. Usually the electronics checkout is the longest, taking from two to three weeks. After this, the instrument is placed on a limited crew access status, to preserve the validity of the checkouts and alignments. A "simulated flight" is performed during which all functions of the experiment are exercised, and the instrument is operated for an appreciable fraction of the expected flight duration. All failures and anomolies are noted, and any repairs or replenishments needed are performed immediately after the simulated flight. In most of our field operations, the requisite repairs or changes were not extensive enough to require a second simulated flight. After completion of these tasks, we hold a "flight readiness review" in which members of the flight team report on the performance of all subsystems, and where possible anomalies are discussed. Until fairly recently, these reviews were attended by non-group experts (from the Johnson Space Flight Center) who questioned the procedures and test results. After the review, the instrument is certified as being ready for flight, and is closed up for the final time. Vital functions such as internal pressures and temperatures are monitored between this time and flight, and expendables such as spark

chamber gas, cryogenic fluids, and external power are replenished from outside as required.

Space shuttle operations will take longer, since there will be much more of an interface with the shuttle support systems than in our nearly self-sufficient balloon gondola. We expect that the checks of our own instrument can be interleaved with these external interface tasks. A typical crew averaged over the nine month's integration period will probably be about 3 full time equivalents, although the number at any given time will fluctuate. The magnet should be operable for interferance tests during all but about the first month of this time period. Limited outside personnel access, as described in Section III E, will be in force at any time the magnet operates and the outside pressure shell protecting the spectrometer is removed. The shell should be removed for most of the time during the first four or five months, but be in place for most of the time following this.

We are not presently aware of any fundamental reason why the magnet could not be launched in an energized state. Even so, we plan to launch in a discharged state, in order to minimize the risk of an unwanted transition during the high stresses of the launch period. After the shuttle has achieved its orbit, the experiment will perform some magnet-off calibrations before turning on the magnet. These calibrations should occupy only two or three orbits. Then, the magnet will be energized, a procedure which takes typically two to four hours. At first, when the current in the coils is low, the current is increased quite rapidly by placing typically six volts across the coils. This energizing rate continues until the current has reached typically 3/4 of the final desired value. The energizing voltage is then reduced substantially for the remainder of the energizing, to minimize the risk of an unwanted magnet transition to a normal (non-superconducting)

state. If such a transition were to occur, a relief valve would vent the excess pressure outside of the dewar. It is not known whether enough liquid helium would remain to permit a second try, but if a second valve were closed beyond the relief valve after the pressure transient had abated, and the relief valve were warmed up with an external heater it probably would re-seat. This would curtail any further loss of liquid helium, and probably would permit the achievement of full flight objectives, since the lifetimes for cryogenics in table 4 are generously larger than the shuttle flight duration. Furthermore, the magnet coils have been designed to reduce the probability of this to an acceptably low level. Magnet energizing could take place either using crew support, or by command from the ground.

Once the magnet is energized, the main data-taking begins. In the early stages of the flight there may be numerous commands which allow recording data in each of the several modes the equipment has available. After this initial phase, however, the data-taking should settle into a pattern with very few alterations until the end of the mission is near.

At this time, the magnet is de-energized, with the stored energy being transferred to an external heat sink through discharge diodes. Discharge typically takes about one hour. When this is completed, we will probably repeat the calibration sequence that took place at the beginning of the flight before the magnet was energized, and then power down the experiment for landing.

VII. Descriptors

Tables 6 - 8 provide experiment descriptors.

VIII. Costs and Schedules

A breakdown of estimated costs is itemized below. A tacit assumption has been the exclusion of all R&QA costs not required by a level of effort equivalent to a balloon program. We see the Shuttle as a manned vehicle where limited changes or corrections can be accomplished during flight. The flight opportunities on Shuttle are also of great frequency compared with a once-only free-flyer mission. We therefore emphasize that considerable cost savings can be realized if the need for documentation is relaxed well below that required for previous free-flyer missions, and the costs below are estimated on this basis. Further cost reductions were realized from our HEAO-B program by the cryostat redesign commensurate with the shorter helium lifetime required and a minimum-cost constraint. Costs for other subsystems (spatial detectors, electronics, ...)are only estimates, since such systems were not addressed in this study. The spatial-detector costs will roughly double if a second spectrometer is added to the other end of the cryostat. Program management will be directed by our own group.

The overall schedule is judged to be two to three years, based on the experience gained from both our balloon program and the fabrication of our HEAO-B thermal model cryostat. Little development time is anticipated, except possibly for other subsystems which might be added to the basic spectrometer for a particular experiment goal (e.g., transition radiators, a total-absorption shower counter, or other detectors for an electron-positron experiment). No additional time has been allocated for documentation over and above that required by NASA for its balloon and rocket programs.

TABLE 6

Orbiter-Spacelab Support Descriptors

Experiment	Space Shuttle magnetic spectrometer
Weight	1230 kg
Size and Shape	Cylinder, 1.6 m dia x 3.8 m long (3.0 m long with only one spectrometer)
Orbit	
a) altitude	N.A.
b) inclination	$\geq 50°$
Pointing/Viewing Requirements	
a) field of view	typically $\pm 30°$ from normal to apparatus
b) accuracy	$\pm 2\frac{1}{2}°$ *
c) stability	N.A.
d) aspect accuracy	$\pm 2\frac{1}{2}°$ *
e) targets in priority order w/viewing time	away from earth
Power Requirements	
a) magnet	100 A power supply for magnet energizing: energizing starts at 6 V but is reduced below 2 V at about 80 amps. Total time: 2-4 hours.
b) other electronics	100 W (est.)
Data Requirements	
a) rate	700 bits/event
b) real time	data dump once per orbit
c) commands	≤ 2 K bits/orbit
d) stored data volume	$\sim 10^9$ bits
Mechanical Systems	pallet mounted
Special Requirements	Pressurized Can, acoustic attenuator
Special Safety Requirements	possible emergency vent procedure if transition occurs during magnet charging.

* Nominal spacecraft pointing information should be adequate for almost all charged cosmic ray studies.

TABLE 7

Environmental Descriptors

Thermal	
a) acceptable	0 to 40° C
b) generated	100 watts (est.)
Vibration	
a) acceptable	Minimum
b) generated	Negligible
Acoustic	
a) acceptable	Minimum
b) generated	Negligible
Electromagnetic Radiation	
a) acceptable	TBD
b) generated	None
Chemical Contamination	
a) acceptable	not critical
b) generated	vent He at 3 Kg/hr during energizing or de-energizing magnet; 0.07 Kg/hr otherwise.
Magnetic Fields	
a) acceptable	Nominal Earth
b) generated	see figure 2
Trapped/Nuclear Radiation	
a) acceptable	$<6 \times 10^6$ Protons/cm^2
b) generated	None

TABLE 8

Operational Descriptors

Initial Prep Time	TBD	
Turn Around Time Between Missions	6 mo to 1 year	(few weeks in the event of an immediate re-flight)
Pre Flight Support Requirements	TBD	
Ground Support Equipment	TBD	
Integration Support		
a) Hardware	Pallet, etc.	
b) Software	Minimal	
Testing (Test Plans, Repts and Reviews)	Thermal, Acoustic and Vibration Test facilities, mag. interference with other experiments	
In Flight Support Requirements	Facilities for Real time Data analysis and telemetry link. Possible crew support for energizing and de-energizing magnet.	
Post Flight Support Requirements	Data Tapes, Bonded Storage Thermal Control	

IX. Future Studies

There are a number of areas for the magnetic spectrometer which need further study, and were beyond the scope of the present work. Although it is likely that no fundamental problem exists, there should be a more detailed investigation of the mechanical connection between cryostat and pallet. The cryostat design could be less conservative if the energy balance for a magnet transition (Section II C4) were better known through further tests with the thermal model cryostat. More testing should be performed to determine whether a magnet coil's charging performance would be better in zero-G if the coil were potted. A comprehensive study of complete electronics needs would certainly be appropriate before proposing a specific experiment for the shuttle, although, as we have observed, the electronics needs probably are not very different from any other cosmic ray instrument employing spatial detectors.

The cryostat investigations described in this report were carried out by Bill Pope with the assistance of Jon Aymong. Many useful contributions were made by Charles Orth, Terry Mast, and George Smoot.

52
PAGE INTENTIONALLY BLANK